



ELSEVIER

Atmospheric Research 50 (1999) 105–117

ATMOSPHERIC
RESEARCH

Contrasting features of two tropical summers from satellite observations

M. Abdel Wahab ^{*,1}, H.M.S. Hasanean ¹

International Center for Theoretical Physics, Trieste, Italy

Received 12 December 1996; accepted 28 October 1998

Abstract

Droughts and floods are important events which directly affect African water resources. The causes of droughts occurring in semiarid regions are not yet well understood. Here we investigate features controlling the dry and wet seasons in North African tropical regions. Data used in this study are ISCCP C2 and Nimbus-7 ERB. We found that changes in surface albedo are major parameters effecting dry and wet seasons. Also, surface longwave radiation and cloud radiative forcing are found to be good indicator parameters to diagnose this phenomena. © 1999 Published by Elsevier Science B.V. All rights reserved.

Keywords: Droughts; Floods; North Africa; ISCCP C2; Nimbus-7 ERB

1. Introduction

Tropical African precipitation is largely controlled by the north–south oscillation of the region between the northern and southern trade wind belts, namely, the Inter Tropical Convergence Zone (ITCZ). The ITCZ moves with the seasons, following the Sun. The north–south movement of the ITCZ is the most important feature of the tropical climate system since it largely controls the spatial and seasonal distribution of rainfall (Farmer and Wigley, 1985).

The main objective in this paper is to investigate the relationship of wet and dry season characteristics to many physical factors. In North Africa, the rainfall pattern is mainly a summer one, therefore data for the month of August for both wet and dry years

* Corresponding author. Tel.: +202-567-6839; Fax: +202-572-7556; E-mail: mmawahab@frcu.eun.eg

¹ Permanent address: Department of Astronomy and Meteorology, Faculty of Science, Cairo University, Giza, Egypt.

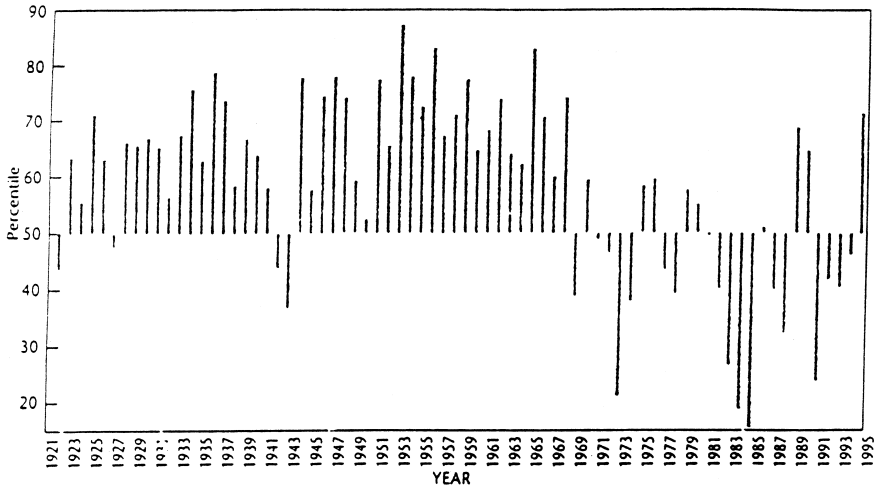


Fig. 1. Precipitation index for the western Sahel for August–September normalized by the 1961–1990 base period (WMO, 1995).

were used to explore causes of differences in the rainfall pattern. The mean summer rainfall is found to be expressed by August. For this reason we take two seasons, one as a ‘drought’ or dry season, August 1983, referred to as Aug83, and the other as a ‘flood’ or wet season, August 1988, referred to as Aug88, over North Africa (see Figs. 1 and 2, WMO (1995, 1984), respectively). Both figures satisfy our selection criteria for ‘wet’ and ‘dry’ summers in terms of the precipitation index and also clear identification of the

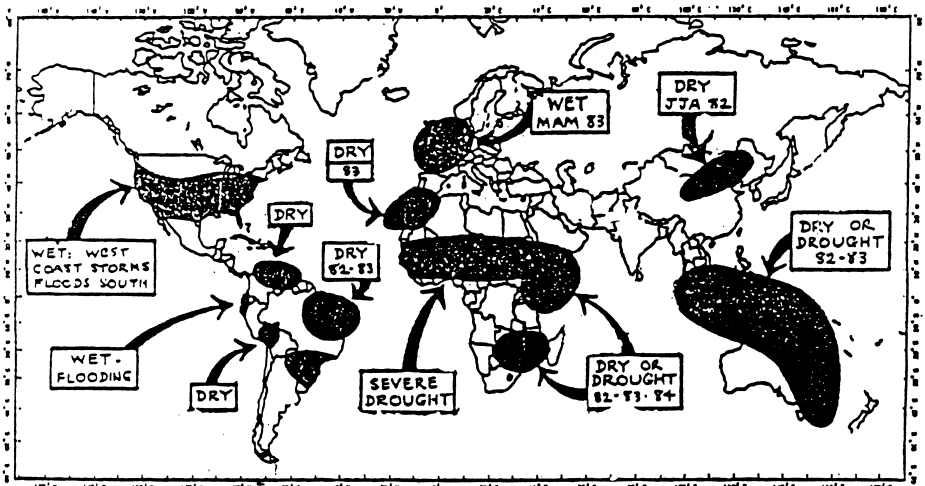


Fig. 2. Selected extreme continental precipitation (wet and dry areas) that persisted for more than a season in the 1982–1984 period (WMO, 1984).

drought at summer 1983. (Our quantitative definition of a 'dry' season is one in which summer precipitation is less than 80% of normal, while a 'wet' season is one in which precipitation greater or equal to 90% of normal precipitation. Precipitation departures are based upon the reference normal period (1951–1970).

This paper is organized as follows: Section 2 discusses the role of radiation parameters, in order to distinguish between wet and dry seasons. In Section 3, cloud radiative forcing terms for both wet and dry season are discussed.

2. Radiation parameters effect

2.1. Surface albedo

Charney (1975) proposed a biogeophysical mechanism to explain climatic variations in terms of radiative fluxes. When vegetation decreases, surface albedo increases. This variation induces more radiative cooling of the air, which induces ascending motion, convective activity, and consequently precipitation. This process, which can occur for large-scale phenomena, is different from the one proposed by Otterman (1974) for a small-scale area. Otterman (1974), who suggested that the denuded surfaces are cooler, when compared under sunlit conditions. This result in a decreased lifting of air necessary for cloud formation and precipitation, and thus lead to regional climatic desertification.

The values of surface albedo in Aug83 are greater than those of Aug88 for each region as shown in Fig. 3a and b respectively, or in a zonal pattern as in Fig. 4a. These results in agreement with many other studies such as Charney et al. (1977), Chervin (1979), Sud and Fennesy (1982), Laval and Picon (1986), and more recently, Dirmeyer and Shukla (1994). They have analyzed the variation of climate due to an increase of surface albedo over different areas.

Fig. 5c and d illustrate latitudinal variations of Aug83 and Aug88, respectively, for middle and high cloud as zonal mean values. These figures indicate that medium and high cloud cover is dominant in tropical regions (observed by International Satellite Cloud Climatology Project ISCCP C2). In general, total cloud cover was found to be smaller in 1983 than 1988. The method of Griffel and Drazin (1981), Fig. 4c, shows that planetary albedo values for Aug88 are greater than those for Aug83 in tropical areas. These results are consistent with other studies suggesting an increase of surface albedo causes a reduction in cloud cover and precipitation and therefore a decrease in the planetary albedo. Recently Dirmeyer and Shukla (1994) explained this relation as the increase of albedo reduced the absorption of solar radiation by the ground. It also reduces the transfer of sensible and latent heat to the atmosphere. This, in turn, causes a reduction in cloud cover (and precipitation) and therefore will lead to a decrease in the planetary albedo.

We have used a single column model, reported by Krishnamurti (1986). The model presents variations in surface albedo upon the net radiation at the base of the atmosphere; estimates of latent and sensible heat fluxes also show this variation. This model provides a method for the calculation of radiative transfer equations. With the aid of this

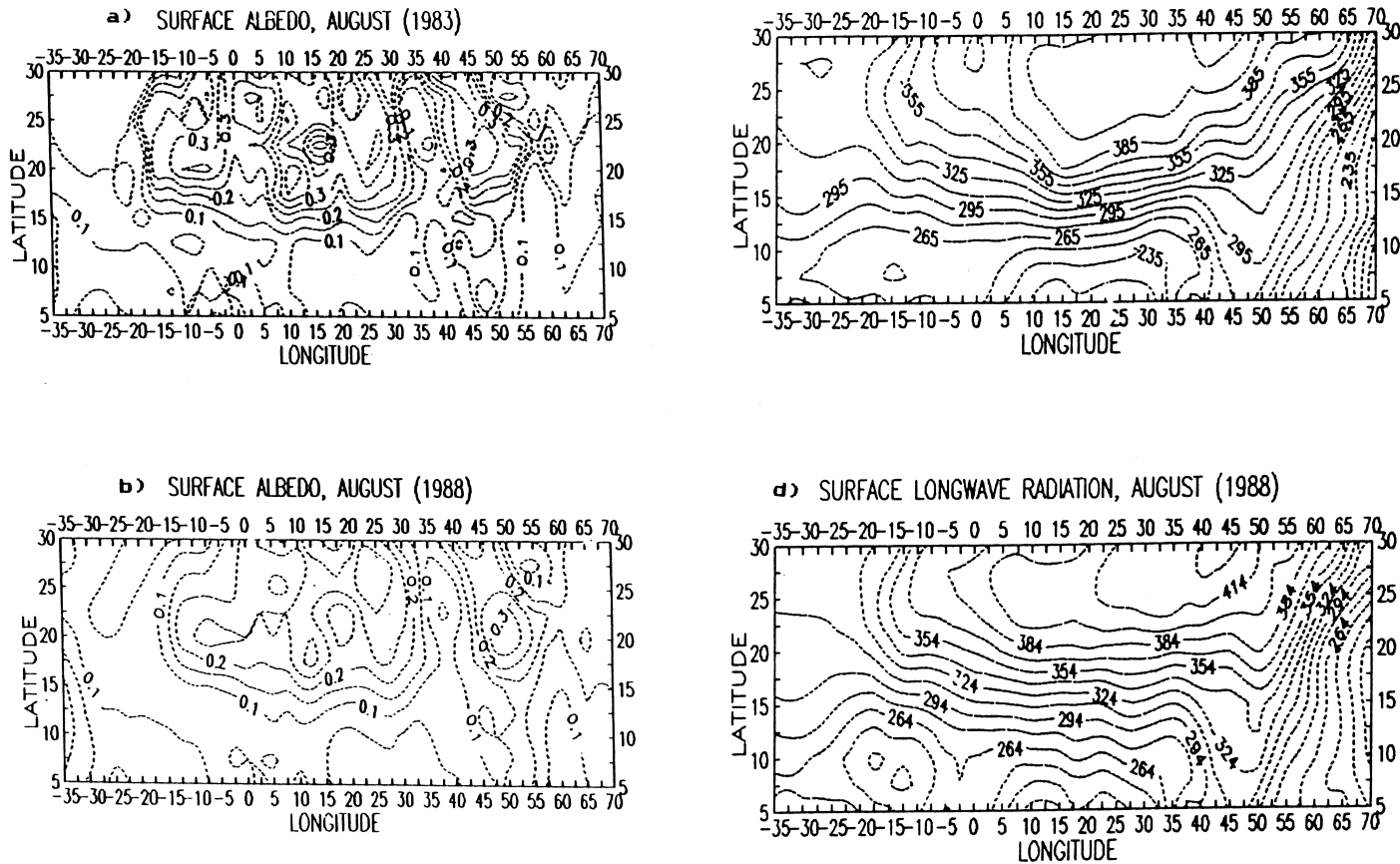


Fig. 3. Regional distribution for (a) surface albedo August (1983), (b) surface albedo August (1988), (c) surface longwave radiation August (1983), surface longwave radiation August (1988).

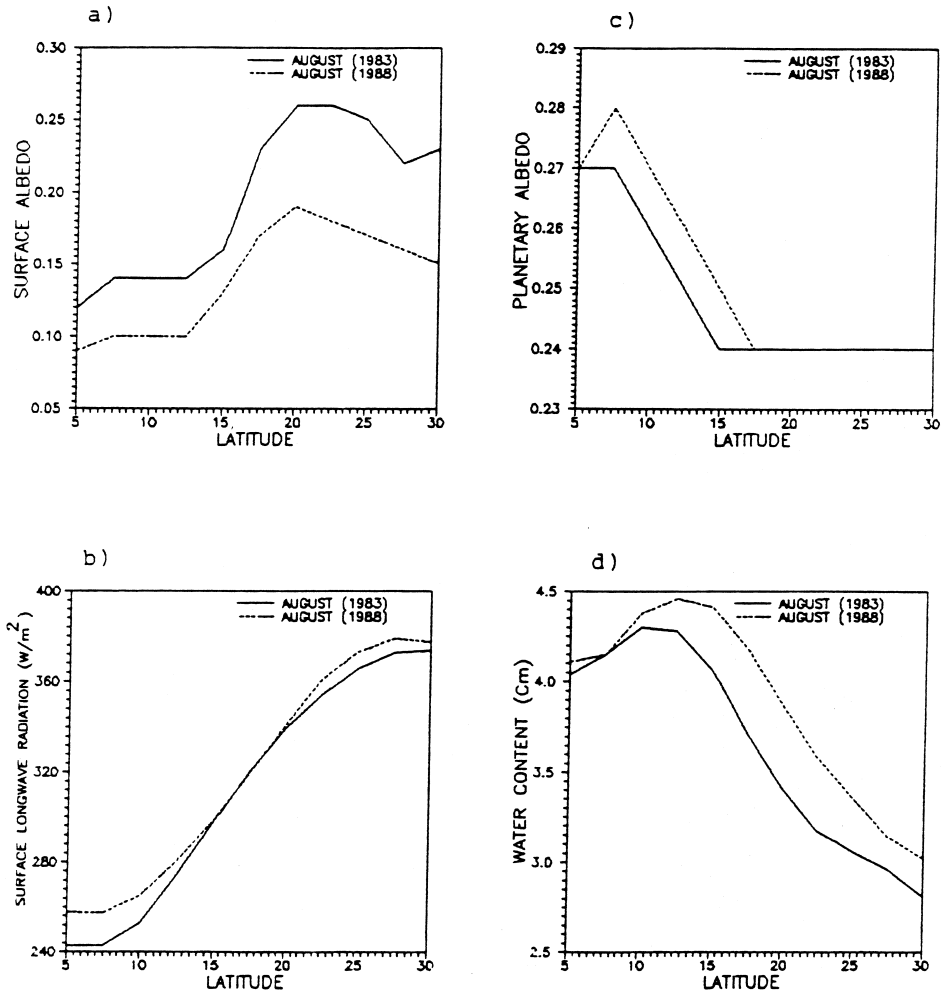


Fig. 4. Zonal variations of August (1983, and 1988) for (a) surface albedo, (b) surface longwave radiation, (c) planetary albedo, and (d) water content.

model, layer and integrated surface fluxes can be estimated. Results from model output in this simulation are presented in Table 1.

Here RN is net radiation at the base of the atmosphere, LE is latent heat, and H is sensible heat. The results indicate good performance by the model and illustrate the role of surface albedo in the system energy balance for a region. Wet-to-dry season transition has associated changes in surface albedo, therefore, the energy budget in the general circulation will vary. These results agree with the result of Charney et al. (1977). He concluded that the increase in surface albedo from 0.14 to 0.35 in semiarid regions induced a decrease of cloud cover. The increase of albedo, and consequently the reduction of the transfer of sensible and latent heat to the air, led to a cooling which

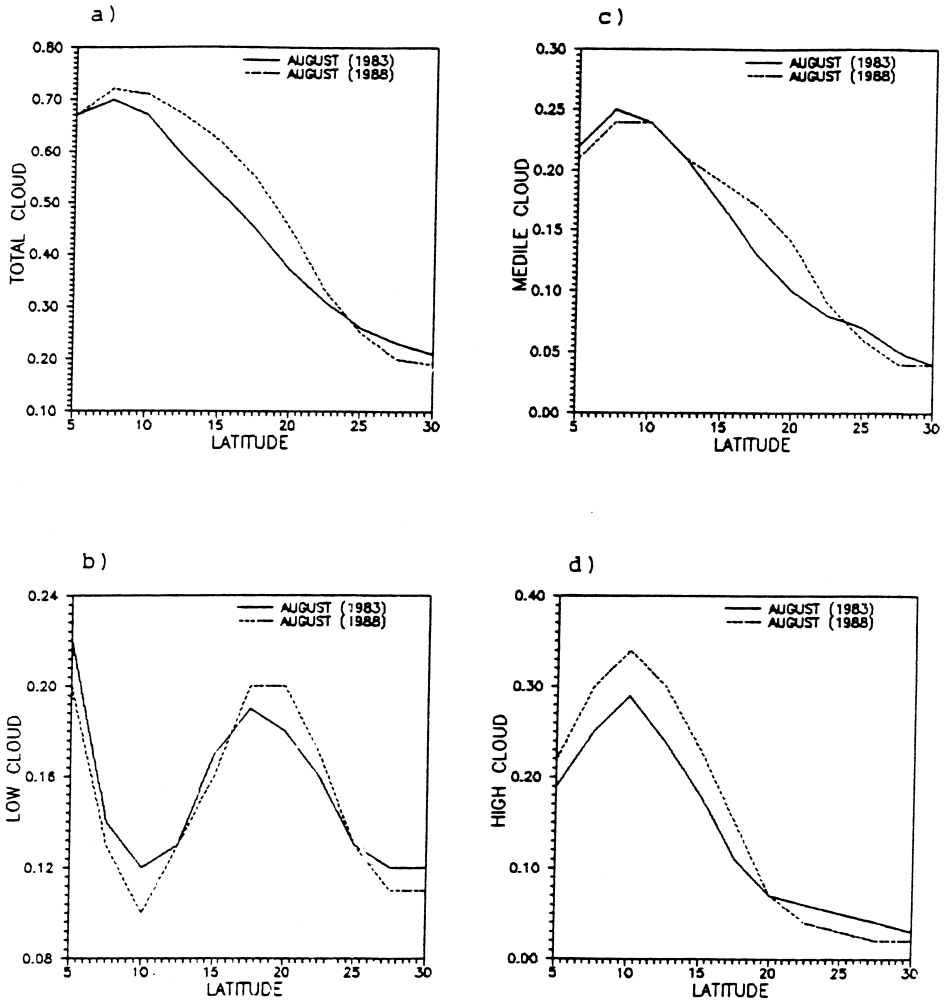


Fig. 5. Zonal variations of August (1983, and 1988) for (a) total cloud amount, (b) low cloud, (c) middle cloud, and (d) high cloud.

either increased low-level horizontal divergence and sinking of air or reduced low-level horizontal convergence and rising. As it is clear that the dynamical and thermodynamical effects supported one another.

Table 1
Relation between surface albedo α_s , and surface fluxes

α_s	RN	LE	H (W/m^2)
0.2	140.6	102.3	35.3
0.3	113.7	85.4	27.1

2.2. Surface longwave radiation

The surface outgoing longwave radiation, OLR_{BOA} , apart from being used as a component of the radiation balance, has proved to be useful for studies of the large-scale circulation over the tropics, e.g., Heddinghaus and Krueger (1981). This is because in the tropics it is largely modulated by the cloudiness.

Fig. 3c and d illustrate the regional distribution of OLR_{BOA} estimated by the method of Adem (1967) for Aug83 and Aug88, respectively. From this figure we see that the Inter Tropical Convergence Zone for Aug88 was at 15°N latitude, while in Aug83 the ITCZ was at 10°N latitude. As shown in Fig. 3c and d, the values of OLR_{BOA} for Aug88 are greater than the corresponding ones for Aug83, especially at the ITCZ. The zonal average of OLR_{BOA} shown in Fig. 4b indicates that the values of OLR_{BOA} for Aug88 are greater than the values of OLR_{BOA} for Aug83 in tropical regions up to 15°N latitude, and approximately equal from 15°N to 20°N latitudes.

The relationship between OLR and surface albedo is an inverse one, as can be seen from Fig. 4a and b, i.e., for Aug83 surface albedo is higher than for Aug88. The corresponding surface longwave radiation OLR is lower for Aug83 than that for Aug88, Fig. 4b. This explains that, as the surface albedo causes a reduction in cloudiness, there was an increase in the net loss of longwave radiation from the ground, since the downward longwave radiation from a cloud (acting as a blackbody at base temperature) is much greater than that from a cloudless atmosphere. As a result, the net absorption of solar plus longwave radiation at the ground was decreased.

3. Cloud radiative forcing factor

The effect of clouds on the radiative fluxes at the top of the atmosphere (TOA), often defined as the difference in the TOA flux between regions of cloudy and clear skies, is called ‘cloud radiative forcing’. It is becoming increasingly evident that clouds play a major role in governing the surface energy balance, affecting the weather and climate through the modification of the radiative heating and cooling profiles in the atmosphere and the modulation of solar insolation at Earth’s surface.

3.1. Cloud radiative forcing estimates

Longwave cloud radiative forcing $C(L)$ is defined as

$$C(L) = L_c - L \quad (1)$$

where L_c is clear-sky longwave flux and L is absorbed total longwave flux at the top of the atmosphere. The formula of Blanchet (1990) for the longwave cloud forcing can be written as

$$C(L) = e_c \sigma A_c (T_s^4 - T_c^4) \quad (2)$$

where e_c , A_c , T_s and T_c are cloud emissivity, cloud amount, surface temperature, and cloud temperature, respectively. The emissivity factor, e_c , is taken as unity for sake of simplicity.

Similarly, cloud radiative forcing for shortwave flux $C(K)$ is

$$C(K) = K_c - K, \quad (3)$$

where K_c and K are clear-sky and cloudy shortwave radiation, respectively. These can be written as

$$K = S(1 - \alpha) \quad (4)$$

and

$$K_c = S(1 - \alpha_s). \quad (5)$$

$C(K)$ can then be written from Eqs. (4) and (5) as

$$C(K) = S(\alpha - \alpha_s), \quad (6)$$

where S is the ‘mean solar insolation’ for the region of interest, α is the planetary albedo and, α_s denotes the observed clear-sky albedo. Net cloud radiative forcing $C(N)$ is then

$$C(N) = C(L) - C(K) \quad (7)$$

We have used the data of Nimbus-7 Earth Radiation Budget ERB compiled with ISCCP C2 data to calculate the three terms of $C(L)$, $C(K)$ and net $C(N)$ radiative forcing.

3.2. Cloud radiative forcing analysis

Long and short wave cloud radiative forcing is used to diagnose the role of clouds in the climate system, e.g., Ramanathan et al. (1989), and Harrison et al. (1990). The regional distribution of shortwave and longwave cloud radiative forcing from satellite data for Aug83 and Aug88 are presented in Fig. 6. The SW cloud forcing produced strong cooling over the Inter Tropical Convergence Zone (ITCZ) for both months. In contrast, a maximum of LW cloud forcing is found over the ITCZ and consequence LW cloud forcing produced strong warming over ITCZ for both seasons. The large magnitudes of SW cloud forcing exist over much of the ITCZ and compensate appreciably for large values of LW cloud forcing. From Fig. 6 we can see that where cloud radiative forcing is present, based on the maximum LW cloud forcing, the ITCZ for Aug88 shifted northward up to 15°N latitude along (5 E–35 E) longitude. On the other hand, in Aug83 the ITCZ has been shifted only up to 10°N latitude. The order of the negative SW cloud forcing for Aug83 at ITCZ area is smaller than SW cloud forcing for Aug88, as appears from Fig. 6a and b for Aug83 and Aug88 respectively. Comparing the Fig. 6c and d, the longwave drop in Aug83 is smaller than in Aug88. Similar results have also been obtained by Ramanathan et al. (1989) for severe drying of the mid-continental regions in North America and Europe. According to Manabe and Wetherald (1987), the decrease could be as much as 25 W/m², as in our results over tropical region. Ramanathan et al. (1989) explained these observations as an initial tendency for drying causes a decrease in cloudiness, which leads to an increase of solar heating of the soil. This amplifies the tendency toward drying. This positive cloud feedback mechanism implies that the size of the negative SW cloud forcing would decrease significantly during a drought event.

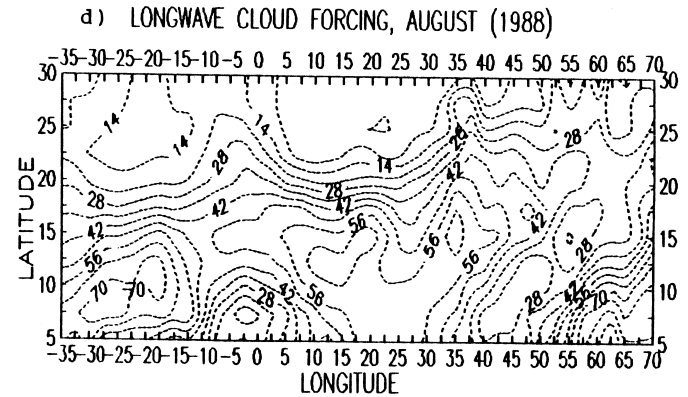
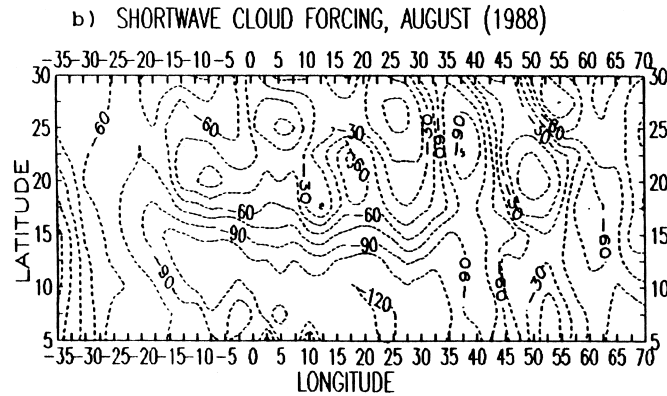
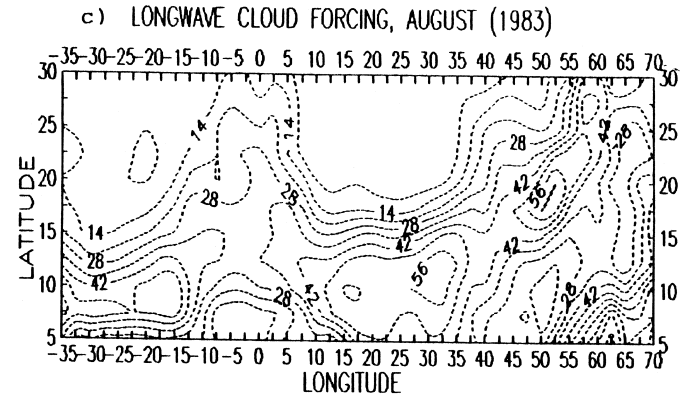
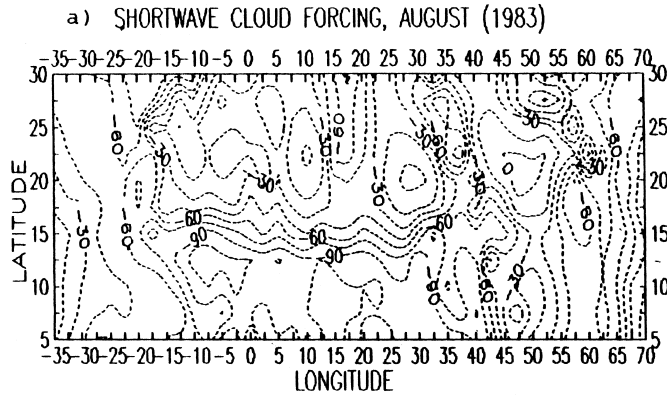


Fig. 6. Regional distribution for (a) shortwave cloud forcing, August (1983), (b) Shortwave cloud forcing, August (1988), (c) longwave cloud forcing, August (1983), and (d) longwave cloud forcing, August (1988).

From Fig. 7 (for zonally cloud radiative forcing), we see that the values of LW cloud forcing for Aug88 are greater than similar ones for Aug83 in the tropical region. This suggests that the heating rate due to clouds in 1988 was more than the heating rate in 1983. This is due to frequent occurrences of high cloud during the wet season. But the values of SW cloud forcing in the wet season, (Aug88), are less than values of SW cloud forcing, in dry season, (Aug83). This is due to the influence of surface albedo in the dry season. The values of net cloud radiative forcing for Aug88 are greater than the corresponding ones for Aug83 up to 17.5°N latitude. This also can be explained by season 1988 having more cloud cover than season 1983. It is important to note that results from Fig. 5 for zonally observed satellite data support this finding. This also

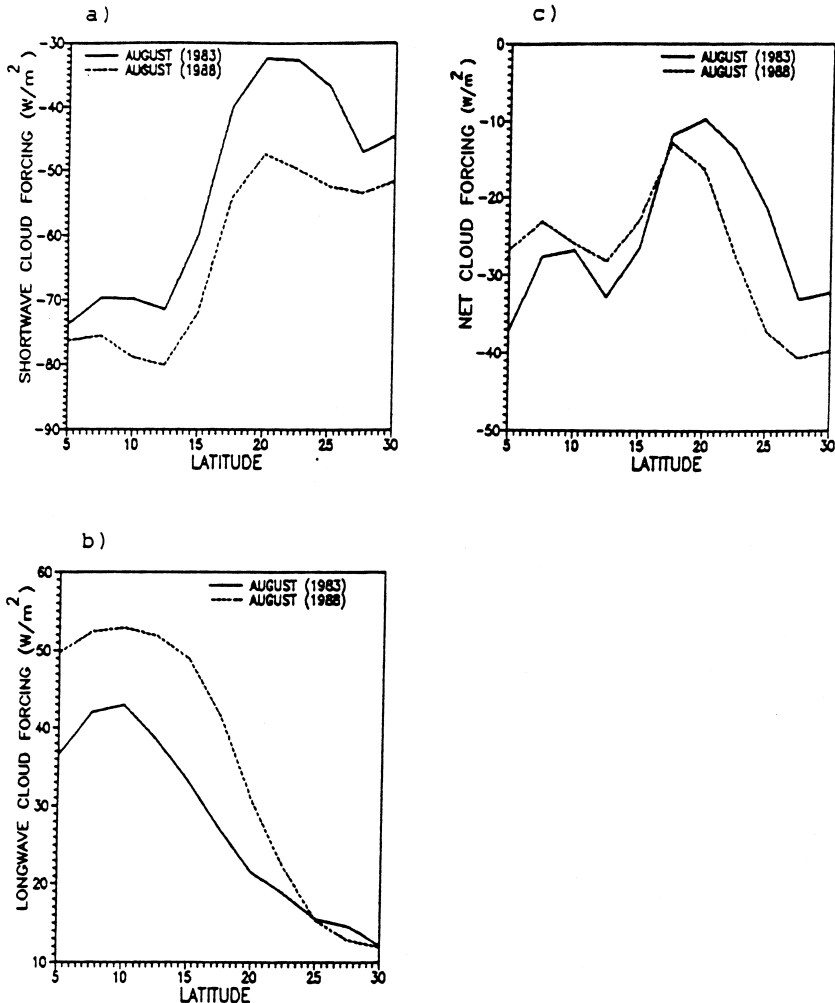


Fig. 7. Zonal variations of August (1983, and 1988) for (a) shortwave cloud forcing, (b) longwave cloud forcing, (c) net cloud forcing.

agrees with previous results. Moreover, we see that the wet season of 1988 has a larger contribution of cloud-greenhouse than the dry season of 1983. Cloud greenhouse simply indicate the role of cloud feedback in increasing global temperature.

In Fig. 8a and b taken at the height of 700 hPa for Aug88 and Aug83, respectively, subtropical high pressure oscillated more eastward in Aug88 than in Aug83. Consequently the Indian monsoon in 1983 is more dominant than in 1988. In other words, the

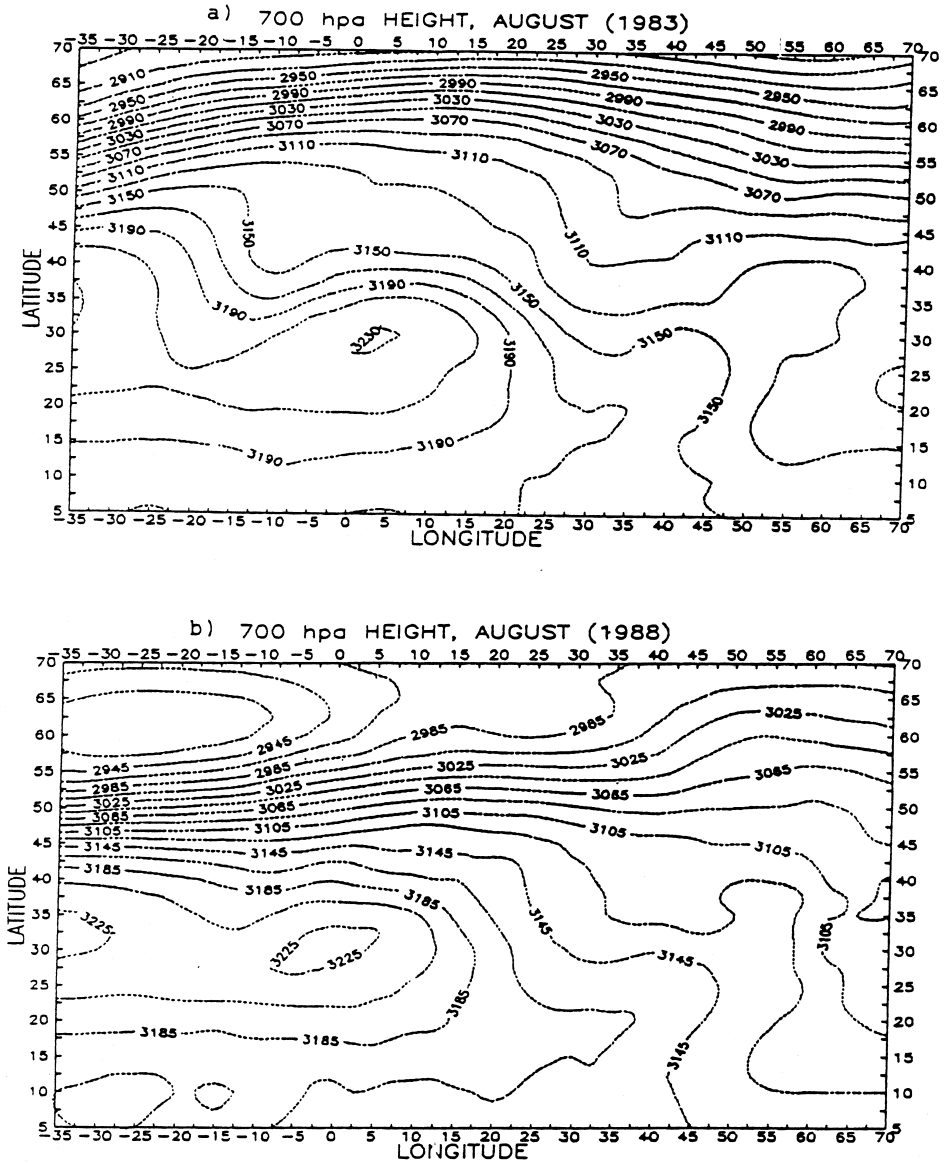


Fig. 8. Contour map of 700 hPa for (a) August (1983), and (b) August (1988).

Indian monsoon in Aug88 was weaker than in Aug83, and hence reduced the cloud fraction. The large-scale tropical circulation system is dominated by the monsoon during the northern summer. The divergent circulations, i.e., local Hadley-type and east–west Walker circulation, associated with the monsoon are substantially strengthened in this season, Chen and Baker (1986). The seasonal movement of the ITCZ is very similar to the seasonal monsoon cycle. The north–south movement of the ITCZ is the most important feature of the tropical climate system since it largely controls the spatial and seasonal distribution of rainfall.

Thus the fact that features of the distribution of LW cloud forcing for Aug88 were different from Aug83 in the tropical region may be due to the effect of Indian monsoon in both seasons.

4. Concluding remarks

This treatment stresses that dryness is related to high surface albedo, and consequently led to low outgoing longwave radiation, low planetary albedo, low cloud amount. The situation is reversed with wetness. Also, dryness of the tropical region may be attributed to the southward oscillation of Indian monsoon. Cloud-greenhouse effects in wet years are more significant than in dry years due to high frequency of high cloud in the tropical region.

Acknowledgements

We would like to thank the reviewers for their useful comments and NASA Langley Research Center EOSDIS Distributed Active Archives Center for providing us the ISCCP C2, National Space Sciences Data Center, NASA Climatology Project and the European Center for Medium range Weather Forecasting (ECMWF) for providing data used in the study.

References

- Adem, J., 1967. On the relation between outgoing longwave radiation, albedo, and cloudiness. *Mon. Wea. Rev.* 95, 257–260.
- Blanchet, J.-P., 1990. Comments on atmospheric feedbacks. In: Manowitz, B. (Ed.), *Global Climate Feedbacks*. Proceedings of the Brookhaven National Laboratory Workshop, June 3–6.
- Charney, J.G., 1975. Dynamics of deserts and drought in the Sahel. *Quart. J. Meteor. Soc.* 101, 193–202.
- Charney, J.G., Quirk, W.J., Chow, S.H., Kornfield, J., 1977. A comparative study of the effects of albedo change on drought in semi-arid regions. *J. Atmos. Sci.* 34, 1366–1385.
- Chen, T.C., Baker, W.E., 1986. Global diabatic heating during FGGE SOP-1 and SOP-2. *Mon. Wea. Rev.* 114, 2578–2589.
- Chervin, R.M., 1979. Response of the NCAR general circulation model to changed land surface albedo. Report of the JOC Study Conference on Climate Models: Performance, Intercomparison and Sensitivity Studies. GARP Publ. Series, Washington, DC, 22 (1) 563–581.

- Dirmeyer, P.A., Shukla, J., 1994. Albedo as a modulator of climate response to tropical deforestation. *J. Geophys. Res.* 99, 20863–20877.
- Farmer, G., Wigley, T.M.L., 1985. Climatic trends for tropical Africa. A Research Report for the Overseas Development Administration. Climatic Research Unit, School of Environmental Sciences, University of East Anglia, Norwich, NR4 7TJ, UK.
- Griffel, D.H., Drazin, P.G., 1981. On diffusive climatology models. *J. Atmos. Sci.* 38, 2327–2332.
- Harrison, E.F., Minnis, P., Barkstrom, B.R., Ramanathan, V., Cess, R.D., Gibson, G.G., 1990. Seasonal variation of cloud radiative forcing derived from the earth radiation budget experiment. *J. Geophys. Res.* 95, 18687–18703.
- Heddinghaus, T.R., Krueger, A.F., 1981. Annual and interannual variations in outgoing longwave radiation over the tropics. *Mon. Wea. Rev.* 109, 1208–1218.
- Krishnamurti, T.N., 1986. Numerical weather prediction for the tropics. WMO, No. 669.
- Laval, K., Picon, L., 1986. Effect of a change of the surface albedo of the Sahel on climate. *J. Atmos. Sci.* 43, 2418–2429.
- Manabe, S., Wetherald, R., 1987. Large scale changes of soil wetness induced by an increase in atmospheric carbon dioxide. *J. Atmos. Sci.* 44, 211–235.
- Otterman, S., 1974. Baring high-albedo soils by overgrazing: a hypothesized desertification mechanism. *Science* 186, 531–533.
- Ramanathan, V., Cess, R.D., Harrison, E.F., Minnis, P., Barkstrom, B.R., Ahmed, E., Hartmann, D., 1989. Cloud radiative forcing and climate: result from the earth radiation budget experiment. *Science* 243, 57–63.
- Sud, Y.C., Fennessy, M.J., 1982. An observational data based evapotranspiration function for general circulation models. *Atmos. Ocean* 20, 301–316.
- WMO, 1984. The global climate system. A Critical Review of the Climate System During 1982–1984. WMO.
- WMO, 1995. WMO statement on the status of the global climate in 1994. WMO, No. 826.